Molecular Crystals and Liquid Crystals Science and Technology. Section A. Molecular Crystals and Liquid Crystals

Publication details, including instructions for authors and subscription information:
http://www.tandfonline.com/loi/gmcl19

Optically Addressed Liquid Crystalline Light Valves - Theory of their Operation and Applications

Andrzej Miniewicz [a], Stanislaw Bartkiewicz [a] & Francois Kajzar [b]

[a] Wroclaw University of Technology, Institute of Physical and Theoretical Chemistry, 50-370, Wroclaw, Poland

[b] LETI - CEA (Technologies Avancees) DEIN/SPE, Groupe Composants Organiques, Saclay, F91191, Gif Sur Yvette, France

Version of record first published: 24 Sep 2006

To cite this article: Andrzej Miniewicz, Stanislaw Bartkiewicz & Francois Kajzar (2000): Optically Addressed Liquid Crystalline Light Valves - Theory of their Operation and Applications, Molecular Crystals and Liquid Crystals Science and Technology. Section A. Molecular Crystals and Liquid Crystals, 353:1, 435-449

To link to this article: http://dx.doi.org/10.1080/10587250008025680

Mol. Cryst. and Liq. Cryst., 2000, Vol. 353, pp. 435-449
Reprints available directly from the publisher
Photocopying permitted by license only

Optically Addressed Liquid Crystalline Light Valves – Theory of their Operation and Applications

ANDRZEJ MINIEWICZ[a], STANISLAW BARTKIEWICZ[a] and FRANCOIS KAJZAR[b]

[a]*Wroclaw University of Technology, Institute of Physical and Theoretical Chemistry, 50–370 Wroclaw, Poland and* [b]*LETI – CEA (Technologies Avancees) DEIN/SPE, Groupe Composants Organiques, Saclay, F91191 Gif Sur Yvette, France*

We report on our research which is focused on developing liquid crystalline optically addressed light valves, their characterization, performances and drawbacks. We study various processes leading to creation of index grating in nematic liquid crystals by incident light. This can be done via molecular reorientation induced by intrinsic photoconductivity of the liquid crystal mixture or by use of semi-transparent photoconducting electrodes containing photochromic dyes. Depending on construction of liquid crystal panels, materials used or even external optical systems several useful optical devices have been constructed, like: phase conjugate mirrors, Fourier optical correlators for pattern recognition, coherent light amplifiers, incoherent-to-coherent light converters, etc. The physical description of these devices must involve the electrical transport properties of liquid crystal used (ion mobilities, photoconductivity, role of dyes and also resistivity of electrode materials, etc.), its optical and mechanical properties (birefringence, order parameter, light scattering, dynamics of molecular reorientation and index profile along the thickness).

Keywords: liquid crystal; spatial light modulator; real-time holography

INTRODUCTION

Tremendous effort in developing optical signal processing technologies resulted in that novel optoelectronic systems have become more and more competitive

with existing electronic data processing technologies. This is possible due to developments of semiconductor laser diodes, 3-D optical data storage materials, photonic-bandgap materials, liquid-crystal spatial light modulators (2-D input devices) and solid-state detector arrays (2-D output devices).

Materials able to show capabilities of dynamic (reversible) hologram recording and erasing are in the center of interest for material engineers working in the field of optical data recording and processing. Initially only inorganic crystals exhibiting mysterious photorefractive effect enabling holograms to be written and read by laser beams were exploited. Soon other materials became of interest, like photorefractive polymers, photochromic polymers and glasses and photorefractive liquid crystalline materials. The latter materials which are usually in the form of thin oriented layers are of special interest for optical data processing as the storage of optical data can be realized more effectively in opaque materials. Performance of liquid crystals has been recognized to be competitive with other known materials so various real-time holographic optical devices were demonstrated, like optical processors, coherent light amplifiers, light deflectors, spatial filters, etc.. Optically addressed liquid crystalline spatial light modulators (OA LC SLM) became the key elements in optical devices allowing for pattern recognition, associative memory or moving object extraction.

Light induced processes in liquid crystals

For real-time holographic applications of liquid crystals it is important to induce refractive index changes by incoming spatially modulated light. Using strong light intensities one may exploit third order non-linear optical phenomena of electronic origin [1] or Kerr orientational effect called optical Fredeericksz transition [2-4]. The latter has been discovered by Janossy et al. to be strongly enhanced by a small amount of a dye added to nematic liquid crystal [5-8] (cf. Fig. 1a) which allowed to work with much smaller light

intensities. Refractive index changes of an LC can be induced by molecular trans-cis conformational rearrangements or by photochemical photocyclization processes [9-11] occurring in molecules dissolved in liquid crystals. Obvious are temperature induced changes of an order parameter including induction of phase transition [11] when temperature of an LC approaches that of phase transition.

Extremely important are LC light valves based on nonlocal processes in which interaction of light with LC is mediated by surface or bulk properties of material being in contact with LC, like surface mediated LC alignment [12-15] (cf. Fig. 1c), bulk photocurrent induced director reorientations [16-21] (cf. Fig. 1b) or surface photocurrent induced director reorientations [22] (cf. Fig. 1d). Recently chirooptical LC switches have been described [23].

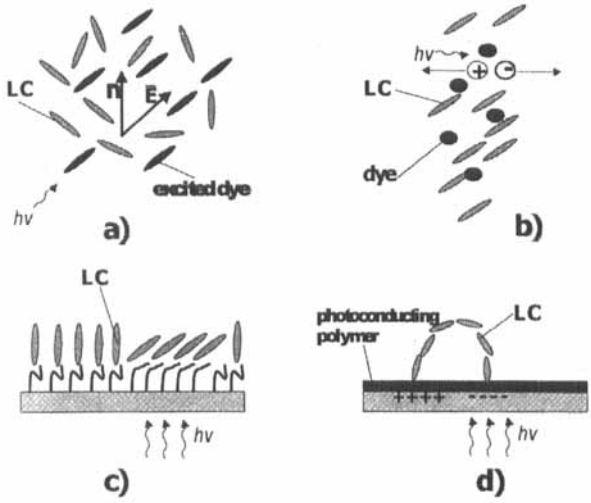

FIGURE 1 Basic ideas explaining various models of light induced refractive index changes in nematic liquid crystals. a) Janossy's model of the dye photoinduced torque; b) bulk photocurrent induced molecular reorientations; c) photo-induced surface command of nematics; d) photoinduced space charge in thin film of polymer serving as orienting substrate.

LIGHT INDUCED SPACE CHARGE FIELDS IN NEMATIC LIQUID CRYSTALS

Uniaxially oriented nematic liquid crystal, when confined between two glass plates with semitransparent electrodes covered by orienting surface layers which impose its homogenous or homeotropic alignment, is a birefringent medium. A unique property of low-molar mass liquid crystal nematics is their ability for local changes of molecular orientation upon electric, magnetic or elastic fields variations as the viscosity of this so called 'soft matter' is relatively small. Let us consider a planarly oriented nematic in which change of an effective $n_e^{eff}(x,y)$ index of refraction for an extraordinary polarized laser beam passing trough a NLC medium along the z direction $n_e^{eff}(x,y)$ is approximated with the following formula [1]:

$$n_e^{eff}(x,y) = \frac{1}{L}\int_0^L \frac{n_e n_o}{\sqrt{n_e^2 \sin^2\varphi(x,y,z) + n_o^2 \cos^2\varphi(x,y,z)}}\,dz \qquad (1)$$

where: L is the thickness of an LC layer, n_e and n_o denote the extraordinary and ordinary refractive indices, respectively. The $\varphi(x,y,z)$ function represents the angular distribution of molecules which are oriented in such a way that the elastic free energy of the system:

$$\begin{aligned} F = &\frac{1}{2}\int\left\{K_{11}(\nabla\cdot\hat{n})^2 + K_{22}(\hat{n}\cdot\nabla\times\hat{n})^2 + K_{33}(\hat{n}\times\nabla\times\hat{n})^2\right\}dV + \\ &-\frac{1}{2}\int\left\{-K_{24}\nabla\cdot(\hat{n}\times\nabla\times\hat{n} + \hat{n}\cdot\nabla\cdot\hat{n})\right\}dV + \\ &-\frac{1}{2}\int\varepsilon_o\Delta\varepsilon(\vec{E}\cdot\hat{n})^2 dV - \frac{1}{2}\int\frac{\Delta\chi}{\mu_o}(\vec{B}\cdot\hat{n})^2 dV + \frac{1}{2}\int W_o \sin^2\phi dS \end{aligned} \qquad (2)$$

is minimized. In the above formula $\hat{n}$ is the nematic director, K_{11}, K_{22}, K_{33} are splay, twist and bend elastic constants, K_{24} is the saddle-splay surface elastic

constant, **E** and **B** are the electric and magnetic fields and $\Delta\varepsilon$ and $\Delta\chi$ are the respective susceptibilities, W_o is the anchoring energy and ϕ is the molecular anchoring angle ($\phi = 90^o$ for planar nematic alignment). The $\varphi(x,y,z)$ function can be calculated within a nematogen theory only for the simplest sample geometries and the simplest static spatial distributions of involved force fields. Due to anisotropy of dielectric susceptibility $\Delta\varepsilon = \varepsilon_{\parallel} - \varepsilon_{\perp}$ electric field applied externally to the cell electrodes or the field arising from the space charge distribution or both of them are able to effectively reorient the molecules in a volume of LC. The strength of electric field and direction of field lines depend on particular cell geometry, electric boundary conditions and light intensity distribution along the sample thickness and within the modulator plane. In real situations when we deal with conductivity and photoconductivity of the liquid crystal the complexity of the problem goes far outside the nematogen theory. For instance, if we introduce a conduction processes in the LC, the dielectric displacement vector $\mathbf{D} = \varepsilon\varepsilon_o\mathbf{E}$ is no longer constant through the cell gap. The inclusion of the correct profile of **D** into the energy expression (eq. 2) links ion transport processes with the orientation of the LC molecules as was considered by Colpaert et al.[24] for pure nematic for which the recombination and generation processes were unimportant. Situation is different when LC has impurities serving as efficient photogeneration species for charge carriers (ions) inside the bulk of the liquid crystal layer. These effects again were considered by several authors [25-28]. An understanding of particular mechanism which is the most efficient for hologram recording for a given LC light valve is not an easy task to do and should always be considered in conjunction with a detailed cell construction and an experimental geometry. Below we describe two cell constructions for OA LC SLM's developed in our laboratory together with description of their unique performances.

Bulk photoconductivity versus surface conductivity LC cells

Let us consider two LC structures as shown in Figure 2.

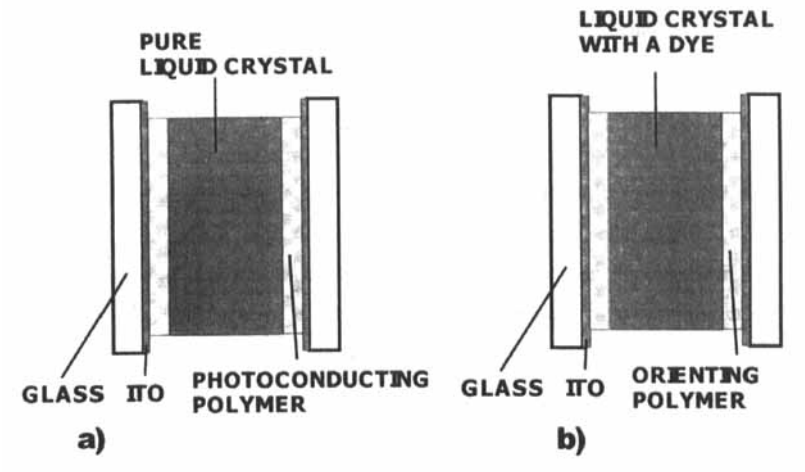

FIGURE 2 A schematic depiction of the two liquid crystal panels described in the present studies: a) hybrid photoconducting polymer - liquid crystal cell, planar configuration; b) planar nematic liquid crystal cell containing an LC doped with an anthraquinone dye.

The layered structure is symmetrically composed of: glass plate, ITO covered glass surface, orienting polymer layer and nematic liquid crystal in the center. For simplicity we assume that both cells have planar configuration of nematic liquid crystal. The main difference between the cells shown above lies in the photoconducting layers. The cell shown in Fig. 2a has the photoconducting layer deposited directly onto ITO glass. As a photosensitive polymer we used soluble polythiophene derivative (cf. Fig. 3a) containing NLO chromophore commercially known as Disperse Red 1 (DR1). This layer simultaneously performs a dual function - that of partially transparent but photoconducting layer and of an alignment inducing layer.[29, 30]

The cell shown in Fig. 2b was filled with nematic mixture containing small amount 0.1 - 1.0% w/w of guest dye molecule of formula shown in Fig. 3 b. Both systems when excited with absorbed laser light at 514 nm or 532 nm show photoconducting properties. In particular under laser illumination at 532 nm and light intensity of 20 $mWcm^{-2}$ a $\frac{\sigma - \sigma_d}{\sigma} = 0.1$ conductivity enhancement in the cell containing a dye was observed [31] (σ and σ_d are photo- and dark conductivities, respectively) . Both systems were carefully studied in our laboratory in respect to their photorefractive properties using a conventional degenerate two-wave mixing technique which is schematically shown in Fig. 4.

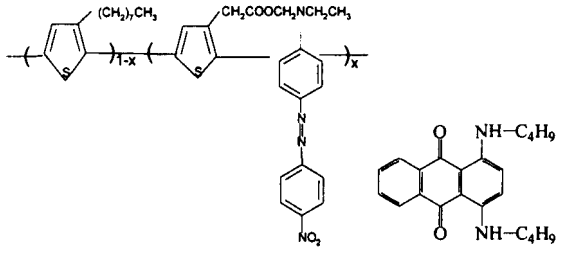

a) b)

FIGURE 3 Chemical structures of the functionalized with Disperse Red 1 polythiophene (a) and of guest anthraquinone dye molecule.

Two coherent p or s-polarized laser beams cross inside the sample and form a simple interference pattern. The spacing $\Lambda = \frac{\lambda}{2n \sin(\theta)}$ of the light intensity grating with the grating wavevector $K = 2\pi / \Lambda$ could be changed by changing the angle 2θ between the two writing beams +0 and -0. In both cases we observed an efficient self-diffraction which is a proof that the system is photosensitive and is able to record light intensity pattern (grating) into

refractive index modulation one. However, diffraction could be observed for hybrid photoconducting polymer - LC sample only at oblique light incidence angle (preferentially Ψ_{tilt} = 45°)[29,30] and with a small wave mixing angle 2θ, no diffraction was seen for Ψ_{tilt} = 0°. Contrary to this for a sample with bulk photoconducting LC layer, light diffraction could be well observed at Ψ_{tilt} = 0° and for any other oblique incidence[31].

Moreover for p-polarized beams in photoconducting polymer - LC sample extremely efficient energy exchange between the inciding beams was possible being dependent on sign of an externally applied voltage. No energy exchange was possible in sample with bulk photoconducting LC layer. We expect that these differences come from differences in refractive index profiles generated by two types of spatial distribution of electric field[32].

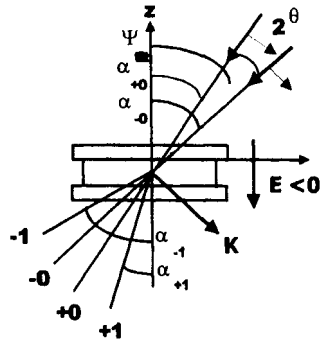

FIGURE 4 Schematic depiction of a degenerate two-wave mixing experiment in a nematic liquid crystal panel.

It is worth of notice that both systems showed similar dynamics of grating recording and erasing. Depending on nematic mixture used and sample geometry the time constants of grating recording and erasing ranged from several ms to several hundreds ms. Light diffraction efficiency in both systems

was usually within few percents but in certain light valves approached value of 30 % which is close to the theoretical limit for thin phase (Δn) gratings.

A BRIEF DESCRIPTION OF GRATING RECORDING MECHANISMS

Light diffraction can be observed when an index of refraction grating is built-up inside a liquid crystal layer. This is possible via action of electric field on particular orientation of molecules. This can be done by efficient light induced charge redistribution inside a thin polymeric layer adjacent to an LC layer or via bulk modification of electric field inside an LC layer by change in resistivity of the layer in dark and bright regions of the crystal, respectively.

Hybrid Photoconducting Polymer - Liquid Crystal Cell

If the incoming sinusoidal light intensity pattern is projected onto a thin photoconducting diffusion and drift of charge carriers occurs polymer as known from description of photorefractive effect. Spatial electric charge density modulation produces a transverse space charge field E_{sc} which is shifted in phase by $\pi/2$ with respect to the light intensity pattern and which is perpendicular to the external electric field E_a . A sum of both these fields induces electric dipole moments of nematic molecules and forms torques τ_E acting on them in order to reorient their long molecular axes along the direction of electric field lines:

$$\tau_E = \frac{\Delta\varepsilon}{4\pi}(\hat{n}\cdot(E_{sc}+E_a))(\hat{n}\times(E_{sc}+E_a)) \qquad (3)$$

where $\hat{n}$ is a director. Both fields depend on the distance z measured inside the liquid crystal layer. A grating which is the result of molecular reorientations in

the simplest case can be described by a modulation of the dielectric permittivity tensor of the liquid crystal at the operation wavelength[33]:

$$\hat{\varepsilon} = < n_c^{eff} >^2 + \hat{\varepsilon}_0^{(1)} + \hat{\varepsilon}_K^{(1)} \left[\frac{E_{+0} E_{-0}^*}{I_0 + I_b} \exp(-iKr) + c.c \right] \tag{4}$$

where $\hat{\varepsilon}_0^{(1)}$ is the spatially homogenous change in permittivity, $\hat{\varepsilon}_K^{(1)}$ is the change in permittivity with spatial frequency K, E_{+0} ,E_{-0} are the complex-field amplitudes of the writing beams, $I_0 = I_{+0}(z=0) + I_{-0}(z=0)$ is the total incident light intensity ($I_{\pm 0} = E_{\pm 0} E_{\pm 0}^*$) and I_b is the background (incoherent) light intensity. The phase mismatch ξ between light intensity grating and refractive index grating leads to efficient energy transfer between the beams. This effect however can be observed only at oblique light incidence. One of the beams experiences gain g at the cost of the second one i.e. if one monitors the -0 beam intensity $I_{-0}(d)$ after the sample without beam +0, and ($I_{-0,+0}(d)$) the intensity of the beam -0 after the sample in the presence of the beam +0 the beam amplification is seen (cf. Fig. 4). The gain parameter *g* can be expressed as[33]:

$$g = \frac{I_{-0,+0}(d)}{I_{-0}(d)} = \frac{1+m}{1+me^{-\Gamma d'}} e^{-\alpha d'} \tag{5}$$

where α is the average absorption coefficient of a liquid crystal at the excitation wavelength, d' is the interaction length and Γ is the exponential gain coefficient:

$$\Gamma = \frac{k_0 \Delta n_K \sin\xi I_0}{(I_0 + I_b)} \tag{6}$$

where Δn_K is the index grating amplitude. The maximum exponential gain coefficient that we observed in the described system at optimal conditions amounted to $\Gamma \cong 2600\ cm^{-1}$ whereas g = 7.

Planar Nematic Liquid Crystal Cell Containing Dye

Another efficient way of mapping the incident light intensity pattern into LC refractive index spatial modulation is to spatially change the electric potential acting on LC layer by means of light. This, in principle, can be achieved with the help of bulk photoconduction process which decreases electrical resistivity of a material in its illuminated regions. The usually nonphotoconductive in the visible spectral range LC's can be sensitized by doping them with the properly chosen molecules enabling photoconductivity e.g. anthraquinone. We have shown that the light valve can operate basing on the bulk photoconductivity current if the LC panel is equipped with a weakly conductive polymeric layer of conductivity comparable to this of LC layer itself. If this is a case one can arrive to a spatial distribution of electric field components E_z and E_x [26] which induce complex molecular reorientations forming index gratings. The main refractive index grating (cf. Fig. 5) which is formed is local (i.e. the phase mismatch $\xi = 0$) with respect to the light intensity pattern and does not allow to observe any energy transfer from beam to beam in a two-wave mixing experiment.

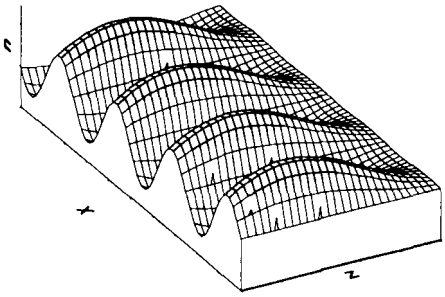

FIGURE 5 A schematic view of the main index grating formed in dye-doped planar nematic liquid crystal as a result of sinusoidal illumination pattern.

The diffraction efficiency defined by the ratio of 1st-order diffracted light intensity to the incident one:

$$\eta = \frac{I_1}{I_o} = |J_1(\phi)|^2 \tag{7}$$

is given by 1st-order Bessel function with effective phase change over sample thickness ϕ given by formula:

$$\phi = \frac{2\pi\Delta n_K d}{\lambda} \tag{8}$$

where Δn_K is the amplitude of modulation of the effective index of refraction in the nematic LC. Diffraction of light on sinusoidal phase grating in the case of thin hologram (i.e. when the condition $Q << 1$ is fulfilled, $Q = 2\pi d\lambda / \Lambda^2 n$), called the Raman-Nath diffraction is attractive for many optical devices because recorded holograms can be reconstructed at any incidence angle.

APPLICATIONS

In recent years we demonstrated how the elaborated by us optically addressed liquid crystalline spatial light modulators could be employed in several useful optical devices. The nature of interaction described above allows to treat these phenomena in terms of real-time holography. In Figure 6 we show the ideas and simplified optical systems realizing the phase conjugate mirror[34] (cf. Fig. 6a), the joint Fourier transform optical correlator for pattern recognition[35] (cf. Fig. 6b), the incoherent-to-coherent image converter (cf. Fig. 6c) and the coherent light amplifier[36] (cf. Fig. 6d). In Fig. 6a the interference of the probe I_p and backward I_b pump beams writes a holographic grating in the LC, which scatters the forward I_f pump in the direction of the conjugate I_c beam. Similarly, the probe and forward pump beams combine to write another grating which scatters the backward pump beam in the direction of the conjugate beam. The maximum phase conjugate reflectivity $R_{PC} = I_c/I_p$ obtained in 15 μm thick LC layer amounted to 2.5 %. In Fig. 6b the object (triangle) and group of various objects are superimposed onto a collimated laser beam I_o by use of an LC transmissive type matrix display. A thin lens performs a Fourier transformation of all the objects which overlap with each other within an LC spatial light modulator.

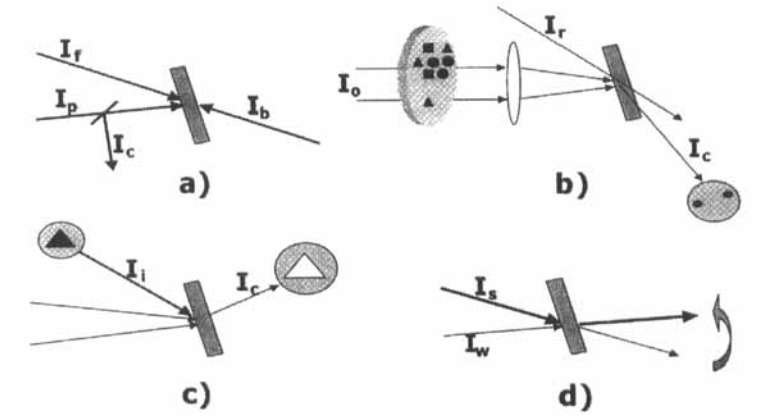

FIGURE 6 Simplified optical systems realizing with the use of optically addressable liquid crystal light valves: a) the phase conjugate mirror; b) the optical correlator for real-time image recognition; c) incoherent-to-coherent image converter and d) coherent light amplifier.

Depending on similarity of Fourier transforms the formation of diffraction gratings takes place. These gratings are read by another laser beam and intensity of first order diffraction (so called correlation peaks) shows correlations between similar or identical objects. The problems which must be solved in this case are connected with spurious light scattering, slow dynamics (40 ms for recognition cycle) and nonlinear modulation transfer function. In Fig. 6c an object (triangle) is superimposed on laser beam I_i which is incoherent with another laser source. The image is projected onto area where two beams not carrying information intersect each other producing simple phase grating inside an LC layer. The diffracted first order light beam I_c carries the information (triangle) if the incoming beam is able to effectively modify the amplitude of the existing phase grating. Finally in Fig. 6 d it is shown how an energy from a strong beam I_s can be transferred to a weak beam I_w by virtue of two-wave coupling process in OA LC SLM. The net gain of an order of 10 can be obtained in 15 μm thick liquid crystal layer[36]. The direction of energy flow can be controlled by the sign of the externally applied voltage.

Acknowledgments

This work was supported by the Polish Committee for Scientific Research through grant no. 3 T09A 04812 and partially within the French-Polish program Polonium.

References

[1] I. C. Khoo, *Liquid Crystals Physical Properties and Nonlinear Optical Phenomena*, J. Wiley, New York (1995).
[2] H. Li, Y. Liang, and I.C. Khoo, *Mol. Cryst. Liq. Cryst.* **251,** 85 (1994).
[3] A. Sugimura, O.-Y. Zhong-can, *Phys. Rev.*, **A 45,** 2439 (1992).
[4] I. C. Khoo, H. Li, and Y. Liang, *IEEE J. Quant. Electron.* **29,** 1444 (1993).
[5] I. Jánossy, *Phys. Rev. E* **49,** 2957 (1994).
[6] I. Jánossy, A.D. Lloyd, and B.S. Wherrett, *Mol. Cryst. Liq. Cryst.* **179,** 1 (1990).
[7] I. Jánossy, L. Csillag, and A.D. Lloyd, *Phys. Rev.* **A 44,** 8410 (1991).
[8] L. Marrucci, *Mol. Cryst. Liq. Cryst.*, **321,** 57 (1998).
[9] B.L. Feringa, W.F. Jager, B. de Lange, *Tetrahedron,* **49,** 8267 (1993).
[10] A.G. Chen and D.J. Brady, *Opt. Letters,* **17,** 441 (1992).
[11] T. Ikeda, O. Tsutsumi, T. Sasaki, *Synthetic Metals* **81**, 289 (1996).
[12] W. M. Gibbons, P.J. Shannon, S.-T. Sun, and B.J. Swetlin, *Nature* **351,** 49 (1991).
[13] A.G.-S. Chen, and D.J. Brady, *Opt. Letters,* **17,** 1231 (1992).
[14] K. Ichimura, in V.P. Shibaev (Ed.) *Polymers as Electrooptical and Photooptical Active Media,* Chapter 4, Springer-Verlag, Berlin (1996).
[15] H. Knobloch, H. Orendi, B. Stiller, M. Büchel, W. Knoll, T. Seki, S. Ito, L. Brehmer, *Synthetic Metals,* **81,** 297 (1996).
[16] I. C. Khoo, *Optics Lett.* **20**, 2137 (1995).
[17] G.P. Wiederrecht, B.A. Yoon, M.R. Wasielewski, *Science,* **270,** 1794 (1995).
[18] A. Miniewicz, S. Bartkiewicz, A. Januszko and J. Parka, p. 487. in F. Kajzar, V. M. Agranovich and C. Y.-C. Lee (eds.), *Photoactive Organic Materials Science and Application,* NATO ASI Series, Vol. **3/9,** Kluwer Academic Publishers, Dordrecht, (1996).
[19] S. Bartkiewicz, A. Miniewicz, A. Januszko and J. Parka, *Pure and Applied Optics,* **5,** 799 (1996).
[20] A. Miniewicz, S. Bartkiewicz, W. Turalski, A. Januszko *in Electrical and Related Properties of Organic Solids* R.W. Munn, A. Miniewicz and B. Kuchta, (eds.) NATO ASI Series, **3/24,** 323, Kluwer Academic Publishers, Dordrecht (1997).
[21] S. Bartkiewicz, A. Miniewicz, *Advanced Materials for Optics and Electronics,* **6,** 219 (1996).
[22] S. Bartkiewicz, F. Kajzar, A. Miniewicz and M. Zagórska, *Appl. Opt.,* **37,** 6871 (1998).
[23] B.L. Feringa, N.P.M. Huck, A.M. Schoevaars, *Adv. Mater.*, **8,** 681 (1996).
[24] C. Colpaert, A. De Meyere, B. Verweire, *Proc. Euro Display'96,* 325 (1996).
[25] E.V. Rudenko, A.V. Sukhov, *JETP (in Russian),* **105,** 1621 (1994).
[26] S. Bartkiewicz, A. Miniewicz, *Adv. Mat. Opt. Electron.*, **6,** 219 (1996).
[27] I.C. Khoo, B. D. Guenther, S. Slussarenko, *Mol. Cryst. Liq. Cryst.*, **321,** 419 (1998).
[28] G.P. Wiederrecht, B.A. Yoon, M.R. Wasielewski, *Science,* **270,** 1794 (1995).
[29] A. Miniewicz, S. Bartkiewicz, F. Kajzar, submitted to *NATO ASI Series,* Kluwer Academic Publishers (1999).
[30] A. Miniewicz, S. Bartkiewicz and F. Kajzar, *Nonlinear Optics,* **19,** 157 (1998).
[31] A. Miniewicz, S. Bartkiewicz, A. Januszko and J. Parka, *NATO ASI Series,* **3/9,** 487, Kluwer Academic Publishers, Dordrecht 1996.
[32] S. Bartkiewicz, F. Kajzar and A. Miniewicz, *Photonics Science News,* **3,** 22 (1998).
[33] A. Miniewicz, S. Bartkiewicz and F. Kajzar, *SPIE Proc.*, **3474,** 172 (1998).

[34] A. Miniewicz, S. Bartkiewicz, J. Parka, *Opt. Commun.,* **149,** 89 (1998).
[35] S. Bartkiewicz, P. Sikorski, A. Miniewicz, *Opt. Lett.* **23,** 1769 (1998).
[36] F. Kajzar, S. Bartkiewicz, A. Miniewicz, Appl. Phys. Lett., in print.